

## Article

# Increased Post-Drought Growth after Thinning in *Pinus nigra* Plantations

Àngela Manrique-Alba <sup>1,\*</sup>, Santiago Beguería <sup>1</sup>, Miquel Tomas-Burguera <sup>2</sup> and Jesús Julio Camarero <sup>3</sup> <sup>1</sup> Estación Experimental Aula Dei (EEAD-CSIC), 50059 Zaragoza, Spain; santiago.begueria@csic.es<sup>2</sup> Centre National de Recherches Météorologiques, Université de Toulouse, Météo-France, CNRS, 31057 Toulouse, France; miquel.tomas@gmail.es<sup>3</sup> Instituto Pirenaico de Ecología (IPE-CSIC), 50059 Zaragoza, Spain; jjcamarero@ipe.csic.es

\* Correspondence: amanrique@eead.csic.es

**Abstract:** In Mediterranean seasonally dry regions, the rise in dieback and mortality episodes observed in pine afforestations has been related to higher drought intensity and lack of appropriate management, which enhance competition between trees for water and light. However, there is little understanding of the benefits of silviculture for plantations under seasonal drought stress. A combination of dendrochronology and wood C and O isotope analyses was used in three Black pine (*Pinus nigra*) plantations to work out the responses of radial growth (BAI, basal area increment) and water-use efficiency (WUEi) to thinning treatments (removal of 40% of the stand basal area). Thinning had a positive effect on BAI and WUEi, reduced drought sensitivity, and reduced the temporal dependence on the previous year's growth. These results were significant even 13–14 years after thinning and coherent for the three study sites. Differences were found between the sites regarding the physiological mechanisms of adaptation. In two sites, we inferred the enhanced WUEi was due to increased photosynthetic rates ( $A$ ) at constant stomatal conductance ( $g_s$ ). In the third site, which had higher tree density and therefore competition, we inferred increases in both  $A$  and  $g_s$ , with the former being proportionally larger than the latter.

**Keywords:** *Pinus nigra*; forest management; water use efficiency; isotopes; dendroecology



**Citation:** Manrique-Alba, À.; Beguería, S.; Tomas-Burguera, M.; Camarero, J.J. Increased Post-Drought Growth after Thinning in *Pinus nigra* Plantations. *Forests* **2021**, *12*, 985. <https://doi.org/10.3390/f12080985>

Academic Editor: Roberto Tognetti

Received: 15 June 2021  
Accepted: 21 July 2021  
Published: 24 July 2021

**Publisher's Note:** MDPI stays neutral with regard to jurisdictional claims in published maps and institutional affiliations.



**Copyright:** © 2021 by the authors. Licensee MDPI, Basel, Switzerland. This article is an open access article distributed under the terms and conditions of the Creative Commons Attribution (CC BY) license (<https://creativecommons.org/licenses/by/4.0/>).

## 1. Introduction

Forests in Southern Europe are expected to undergo severe water limitations and increased temperatures due to climate change [1]. Drought-triggered canopy dieback and mortality have affected some of these seasonally dry forests, such as, for instance, Black pine (*Pinus nigra* Arn.) populations [2,3]. Some studies have reported dieback in Mediterranean tree species, generally viewed as drought-tolerant, such as Holm oak (*Quercus ilex*) [4]. The rise in mortality in some pine forests has also been observed in plantations, and this has been connected not only to increased drought but also to lack of silvicultural intervention (i.e., absence of thinning), which may increase competition between trees for water and light in structurally homogeneous planted stands [3,5].

The knowledge of how forest structure modifies the physiological response of trees to drought would guide managers to implement policies that enhance their resistance against drought. Among other silvicultural options (e.g., species composition), thinning can increase soil water content [6] due to reduced competition [7,8]. Previous research has established that thinning promotes radial growth of the remaining trees in the short and medium terms (1–10 years), with this increase positively correlated with thinning intensity [9]. However, the consequences of rising drought frequency for long-term growth dynamics and the interactions between thinning and post-drought recovery are poorly understood in pine plantations. Furthermore, the tree's response varies with the intensity of the treatment [10], the size [11] and age of the trees [7], the local climate conditions [12], and the period elapsed after the last intervention [13]. For those reasons, there is still

considerable uncertainty about: (i) the optimal thinning intensity, (ii) the duration of thinning effects, (iii) how these effects vary with tree species and local climate. However, to date, most of the available studies have focused on short-term effects. Only a few studies assessed the long-term growth dynamics [14–16].

In addition to growth data, the study of stable isotopes (C, O) in tree-ring wood or cellulose provides insights regarding the tree response mechanisms to drought and thinning [17]. These measures approximate changes in the intrinsic water-use efficiency (WUEi) [18,19]. After a thinning treatment, the response of WUEi is complex, as many studies have shown. Several studies on diverse pine species showed that WUEi decreased after thinning as expected in response to reduced competition for water [20]. Contrary to this, earlier studies have suggested increasing WUEi after thinning [14,21], or even no significant changes [2,22,23]. Thus, the question regarding the effect of thinning on WUEi depends mainly on the tree species and environmental conditions such as climate or stand features such as tree density.

Different physiological adjustments explain WUEi variations after thinning: (i) changes in stomatal conductance ( $g_s$ ) at a steady photosynthetic rate ( $A$ ); (ii) changes in  $A$  at a steady  $g_s$ ; and (iii) changes in both, with that of  $A$  or  $g_s$  being higher. The dual-isotope method has been used to separate the importance of  $A$  and  $g_s$  on WUEi since  $\delta^{18}\text{O}$  is linked to  $g_s$  [24,25]. However, recent studies indicate that this approach has some restrictions and applies only under certain environmental conditions, which should be considered appropriately [26,27].

Our previous research focused on the physiological mechanisms after thinning in an Aleppo pine (*Pinus halepensis*) plantation in dry conditions [28]. We found out that thinning had a positive effect that lasted for almost 20 years. Our results also suggested that changes in water availability were fundamental in improving growth and reducing the growth reliance on adequate climatic conditions. The present study addresses the effect of thinning on a different pine species under less limiting climatic conditions (a mesic site), considering the main environmental conditions modified by thinning (water availability and light).

Therefore, we analysed the long-term response to thinning (thirteen and fifteen years after treatment) in three Black pine plantations located in north-eastern Spain. This shade-intolerant and long-lived pine species is widely distributed across the Mediterranean Basin and central Europe. It is usually very productive in response to wet winter and spring conditions [29], although it is regarded as a drought-tolerant species [3]. However, it can also be periodically defoliated by pine processionary moth (*Thaumetopoea pityocampa*) outbreaks [30].

We used dendrochronology (basal area increment, BAI) and stable isotopes ( $\delta^{13}\text{C}$ ,  $\delta^{18}\text{O}$ ) data to evaluate the climate-growth relationships and the physiological mechanisms of adaptation. We study three sites with similar climatic conditions to determine the robustness of the results. The main issues addressed in this paper were: (i) to evaluate the reaction of BAI and WUEi to long-term thinning and their links with drought intensity, and (ii) to determine the physiological adaptations after thinning driving any changes in WUEi using  $\delta^{18}\text{O}$ .

We hypothesise that thinning will increase BAI and decrease WUEi due to reduced tree-to-tree competition for water. Concerning the physiological mechanisms, we hypothesise that simultaneous analysis of  $\delta^{13}\text{C}$  and  $\delta^{18}\text{O}$  will enable us to identify the relative importance of changes in  $A$  and  $g_s$  on WUEi.

## 2. Materials and Methods

### 2.1. Study Sites and Thinning

We selected three Black pine plantations located in the “Cinco Villas” region in Aragón, north-east Spain (Figure 1): Urriés (42°32' N, 1°05' W, 920 m a.s.l.), Los Pintanos (42°30' N, 1°02' W, 907 m a.s.l.), and Monte Alto (42°33' N, 1°06' W, 705 m a.s.l.). Similar climatic conditions characterise the sites [31,32]. Following the Köppen classification, the climate in the study region is classified as Temperate Oceanic (Cfb) [33]. The mean annual temperature ranges from 11.4 °C in Los Pintanos to 12.2 °C in Monte Alto. The mean annual

Penman-Monteith reference evapotranspiration values are 1069, 1091, 1070 mm in Urriés, Los Pintanos, and Monte Alto, respectively. In contrast, the mean annual precipitation is 907 mm (s.d. of 145 mm) in Urriés, 809 mm (s.d. of 126 mm) in Los Pintanos, and 1060 mm in Monte Alto (s.d. of 178 mm). Therefore, the hydrologic balance is  $-161$ ,  $-10$  and  $-282$  mm in Urriés, Los Pintanos, and Monte Alto, respectively. The maximum rainfall occurs in October in the three sites, with a maximum value of 105 mm in Urriés, 126 mm in Los Pintanos and 93 mm in Monte Alto. Only in Urriés, a period of water shortage occurs in July (Supplementary material, Figure S1).

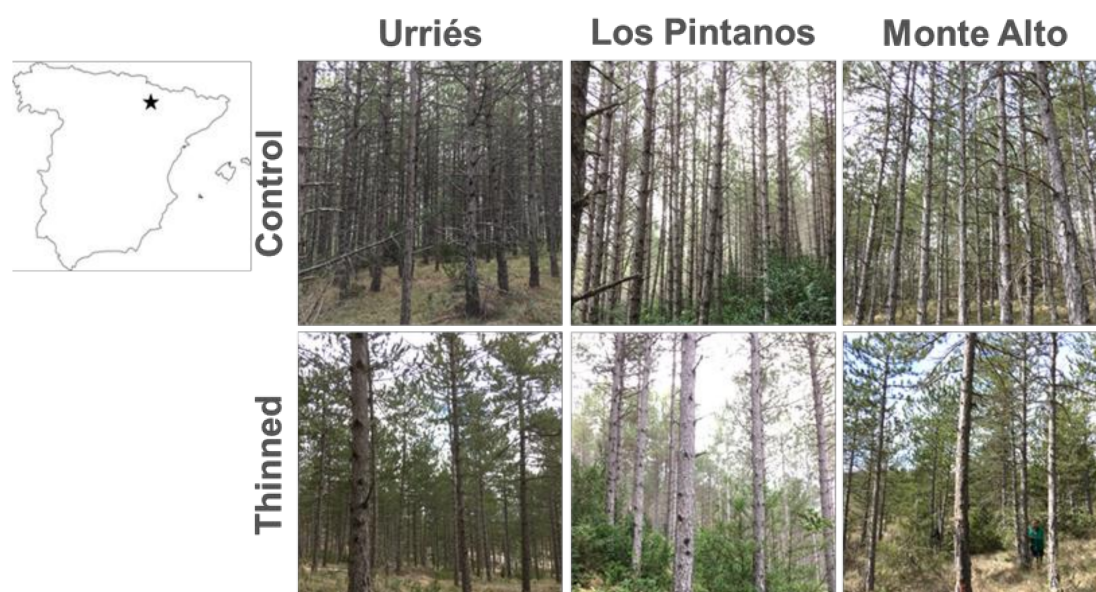


**Figure 1.** Location of the Cinco Villas study area in Aragón, north-eastern Spain, and the control (not-thinned) and thinned plots in the three selected sites. All photographs were taken in the spring of 2019.

Black pine plantations were established in the area during the 1960s with the main objectives of timber production and preventing soil erosion. No forest management was implemented before the thinning trials took place. The plots presented sparse understory vegetation (*Buxus sempervirens* L., *Juniperus communis* L., *Quercus faginea* L. and *Genista scorpius* L.) that was not cleared during the thinning intervention nor after. The slope is between 5–10%. According to the World Reference Base for Soil Resources [34], the soils correspond to Cambisols.

Experimental thinning management occurred in different years. In Urriés, thinning was carried out in 2006, while it was performed in 2000 in Los Pintanos, and 2003 in Monte Alto. The initial canopy cover was similar in the three sites. More precisely, in Urriés the original canopy cover of 80% (control plot, C) was reduced to 42% (thinned plot, T). In Los Pintanos, the initial canopy cover was diminished from 78% (C) to 48% (T), while in Monte Alto, it went from an initial canopy cover of 68% (C) to 41% (T). Approximately 27–38% of the canopy cover was removed, corresponding to a mean reduction in stand basal area of 40% (Table 1). The Los Pintanos site shows a higher tree density than the other sites.

**Table 1.** *Pinus nigra* plots characteristics in the three study sites before and after thinning.

Site/Thinning Treatment	Diameter at 1.3 m (cm)	Tree Height (m)	Canopy Cover (%)	Density (Trees ha <sup>-1</sup> )	Basal Area (m <sup>2</sup> ha <sup>-1</sup> )
Urriés					
Control	15.9	12.8	80	1879	42.0
Thinned	26.5	13.9	42	414	23.1
Los Pintanos					
Control	15.4	12	78	2548	54.8
Thinned	20.4	11.5	48	978	34.5
Monte Alto					
Control	15.3	12.3	68	1783	34.5
Thinned	21	12	41	573	20.5

## 2.2. Dendrochronology: Tree-Ring Width Data

In 2019 we randomly selected ten trees per plot and treatment and obtained two cores per tree at breast height (1.3 m), using two perpendicular directions, using Pressler borers. A sum of 120 cores from 60 trees was obtained and analysed (Supplementary material, Table S1). Samples were extracted from dominant and mature trees with no observable signs of damage. The diameter of all sampled trees and a total height of 5 trees per plot were measured using girth tapes and clinometers, respectively. In addition, one 25 m × 25 m plot was randomly established in each stand, before and after thinning, to measure canopy cover, tree density, and stand basal area (Table 1).

The increment core samples were air-dried, sanded until rings were visible and visually cross-dated. The tree-ring width was measured with a stereo microscope with a precision of 0.01 mm, using the TSAP-Win program LINTAB measuring device (Rinntech, Heidelberg, Germany). The cross-dating quality was examined with the COFECHA program [35]. Ring-width data was converted into basal area increment (BAI), found to be biologically more significant to measure growth differences between years and different treatments [36]. BAI values were computed annually from each ring-width measurement, assuming a circular form of the stems as the variation between consecutive annual cross-sectional basal areas. The mean BAI of the two cores for each tree was considered, and the mean BAI series were used in all statistical analyses. To avoid the use of juvenile trees, data before 1980 were not used.

## 2.3. Climate Data

We used the Standardised Precipitation Evapotranspiration Index (SPEI) to quantify the climatic characteristics (in particular the hydric conditions) during the growing period [37,38]. The SPEI reports deviations in the climatic water balance (precipitation minus potential evapotranspiration) compared to the average conditions at a site, taking positive values for more humid than normal conditions and negative values for drought conditions.

We downloaded SPEI data for the study area from <http://monitordesequia.csic.es> (accessed on 22 May 2021) [31]. The data has a weekly frequency and is available at various time scales (length of the period over which the climatic water balance is computed). Therefore, there are many possible combinations of time scale and calculation period that can be used in the analysis. We carried out a correlation analysis between BAI and the SPEI at different time scales, using the data between the previous year's October and December. This allowed determining the week of the year and the aggregation time scale that presented the highest correlation with tree growth.

## 2.4. Intrinsic Water Use Efficiency (WUEi) and Isotopes Analysis

Wood tissue samples were taken for C and O isotope analyses [39]. According to their good correlation with the mean growth series, five trees were selected in control and thinned plots. Single-year rings were then isolated, and pools of trees were created for each year after 1990 until the present. The samples were milled to a fine powder (Retsch

MM301 mixer mill, Haan, Germany), and 0.001 g aliquots were taken using a micro-balance (AX205 Mettler, Toledo, OH, USA). Samples for  $\delta^{13}\text{C}$  determination were stored in tin foil capsules, while those for  $\delta^{18}\text{O}$  were put in silver foil capsules. Isotopes were analysed at the Stable Isotope Facility of the University of California at Davis (USA).  $\delta^{13}\text{C}$  was determined after combustion to  $\text{CO}_2$  by utilising a Flash EA-1112 elemental analyser interfaced with a Finnigan MAT Delta C isotope ratio mass spectrometer (Thermo Fisher Scientific Inc., Waltham, MA, USA). For  $\delta^{18}\text{O}$ , the samples were combusted in an elementary PyroCube (Elementar Analysensysteme GmbH, Hanau, Germany) interfaced to a PDZ Europa 20-20 isotope ratio mass spectrometer (Sercon Ltd., Cheshire, UK). Stable isotope ratios were represented as per mil (‰) deviations using the  $\delta$  notation relative to VPDB (for carbon) and VSMOW (for oxygen) standards.

We computed C isotope discrimination in wood ( $\Delta^{13}\text{C}$ ) using changes in  $\delta^{13}\text{C}$  of atmospheric  $\text{CO}_2$  ( $\delta^{13}c_a$ ) and wood  $\delta^{13}\text{C}$  ( $\delta^{13}c_w$ ) as:

$$\Delta^{13}\text{C} = (\delta^{13}c_a - \delta^{13}c_w) / ((1 + \delta^{13}c_w) / 1000) \quad (1)$$

$\delta^{13}c_a$  was obtained from McCarroll and Loader [18] and Belmecheri and Lavergne [40].  $\Delta^{13}\text{C}$  results from the preferential use of  $^{12}\text{C}$  over  $^{13}\text{C}$  during photosynthesis and depends on: (i) the fractionation during  $\text{CO}_2$  diffusion through the stomata ( $a = 4.4\text{‰}$ ), (ii) the fractionation by RuBisCO ( $b = 28.0\text{‰}$ ), (iii) leaf intercellular space ( $c_i$ ), and ambient  $\text{CO}_2$  concentrations ( $c_a$ ) [41]. Then, we computed WUEi (in  $\mu\text{mol mol}^{-1}$ ) utilizing the equation suggested by Farquhar et al. [42]:

$$\text{WUEi} = c_a [1 - (c_i / c_a)] 0.625 = (c_a - c_i) / 1.6 \quad (2)$$

where 0.625 is the ratio between the conductance of  $\text{H}_2\text{O}$  in comparison to the conductance of  $\text{CO}_2$ . To define  $c_i$ , we referred Francey and Farquhar [43]:

$$c_i = [(\Delta^{13}\text{C} - a) \times c_a] / (b - a) \quad (3)$$

### 2.5. Statistical Analysis

A generalised linear mixed-effects model (GLMM) [44] was fitted at each site with BAI as the response variable and the previous-year BAI ( $\text{BAI}_{\text{prev}}$ ) and current-year SPEI as fixed effects.  $\text{BAI}_{\text{prev}}$  accounted for temporal autocorrelation often present in tree-ring width data, while SPEI accounted for the drought effect on growth. The data were entered for each sampled tree individually, so the tree identifier was used in the model as a random effect, thus controlling for between-individual variability. The combination of treatment (thinned/control) and period (pre/post-treatment) was used as a factor interacting with the models' intercept and the  $\text{BAI}_{\text{prev}}$  and SPEI coefficients, leading to a total of twelve model coefficients ((intercept + two fixed effects)  $\times$  two treatments  $\times$  two periods).

Due to the nature of the BAI data, which contains only positive values and exhibits a characteristic skewed distribution, the Gamma distribution family with a logarithmic link was used to relate the linear predictor to the conditional mean of the response. The model was fitted via maximum likelihood using the BOBYQUA algorithm [45], as implemented in the `lme4` package in R [46].

The significance of the model coefficients was determined by their confidence range (estimated at  $\alpha = 0.05$ ) not overlapping zero. The significance of the differences between periods (pre- and post- thinning) and between plots (thinned and control) was determined by their ranges not overlapping each other.

Linear models were fitted for WUEi and  $\delta^{18}\text{O}$ , with SPEI and the interaction of treatment and period as covariates. The effect of the previous-year WUEi and  $\delta^{18}\text{O}$  was not included, as there was no sign of temporal autocorrelation on those variables. Similarly, no link function was required, so a Gaussian model with an identity link was used. As the data were pooled across five trees, no individual random effects were included. The models were fit by Ordinary Least Squares using the `lm` function in R [47].

### 3. Results

#### 3.1. Influence of Thinning on Radial Growth

The BAI time series presented consistent results for all treatment plots before thinning. As expected, BAI decreased notably in drought years (e.g., 1986, 1994–1995 and 2012), while it had high values during wet years (e.g., 2014) (Figure 2). Differences in growth between treatments were minor or even not noticeable before thinning but increased notably after thinning in all sites. The largest differences between treatments (+200–300%) occurred around 2014, coinciding with two consecutive humid years.

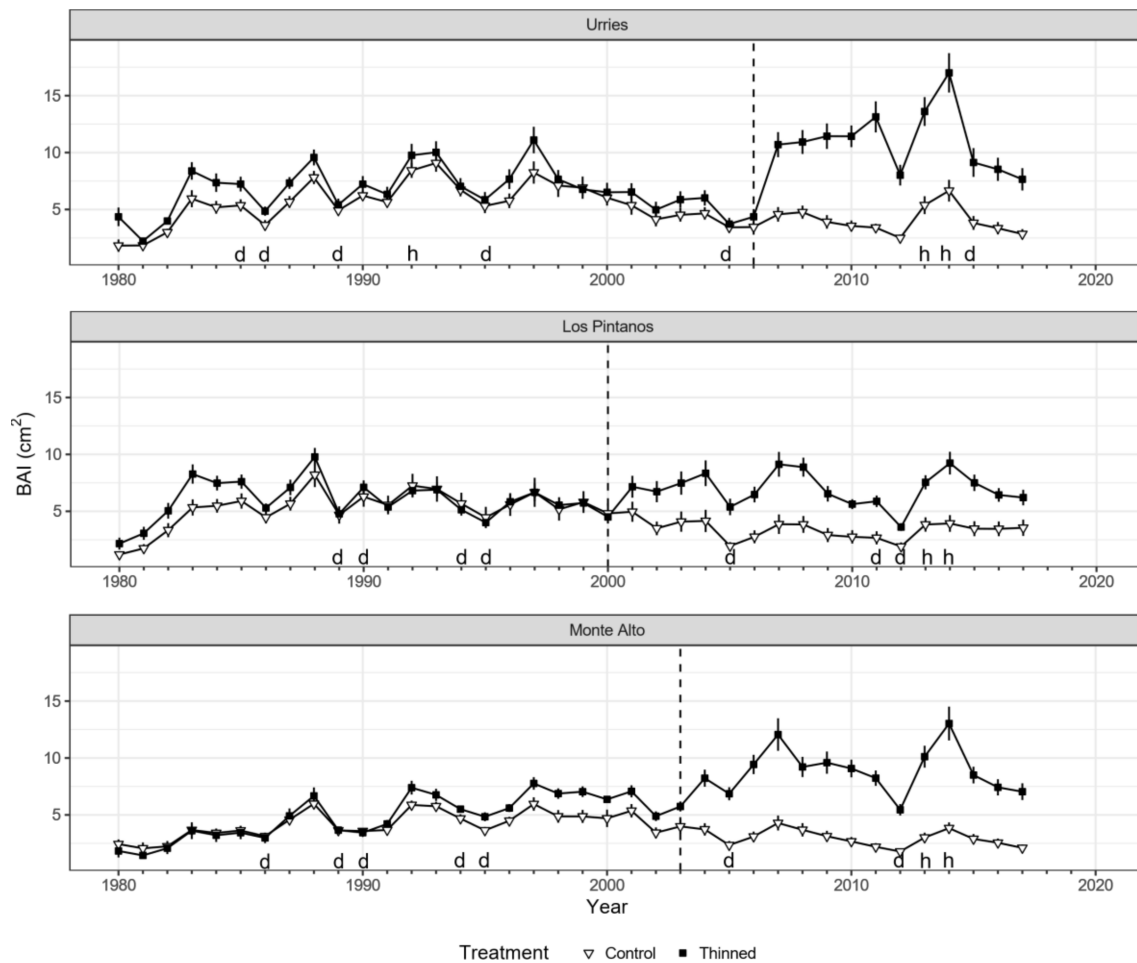


**Figure 2.** Basal area increment (BAI) series of *Pinus nigra* in Urriés, Los Pintanos, and Monte Alto for control plots (black squares) and thinned plots (white triangles). Points represent mean values, while vertical bars depict standard errors. The dashed vertical lines represent thinning treatments (2006, 2000, and 2003 in Urriés, Los Pintanos, and Monte Alto). Letters h and d above the x-axis indicate humid (SPEI > 1.28) and dry (SPEI < −1.28) years, respectively.

#### 3.2. Impact of Climate and Thinning on Growth

The highest correlation between BAI and SPEI series was observed after summer for all sites (Figure S2 in the Supplementary material). More precisely, the highest correlation was at the time scale of 6 months and week 42 of the year (November) in Urriés, with a positive and significant ( $p < 0.05$ ) coefficient correlation of 0.584. In Los Pintanos, it was found in week 37 (early September) at a time scale of 9 months, with a coefficient of 0.565. In Monte Alto, the highest correlation also corresponded to week 37 (early September) at a time scale of 12 months and 0.562 (Figure S3). Consequently, these SPEI data time scales were selected for use in the regression analysis as independent variables for BAI. Additionally, the most severe droughts for each site based on the SPEI data were, 1985–1986,

1989, 1995, 2001 and 2016 in Urriés, 1989, 1994–1995, 2005, and 2011–2012 in Los Pintanos and 1985–1986, 1989, 1995, 2001, and 2016 in Monte Alto (Figure S3).

According to the regression analyses, BAI was significantly influenced by  $BAI_{prev}$  and the SPEI (Figure 3a and Table S2). Comparing model coefficients across the three sites, it can be seen that they were similar, stressing the robustness of the results.

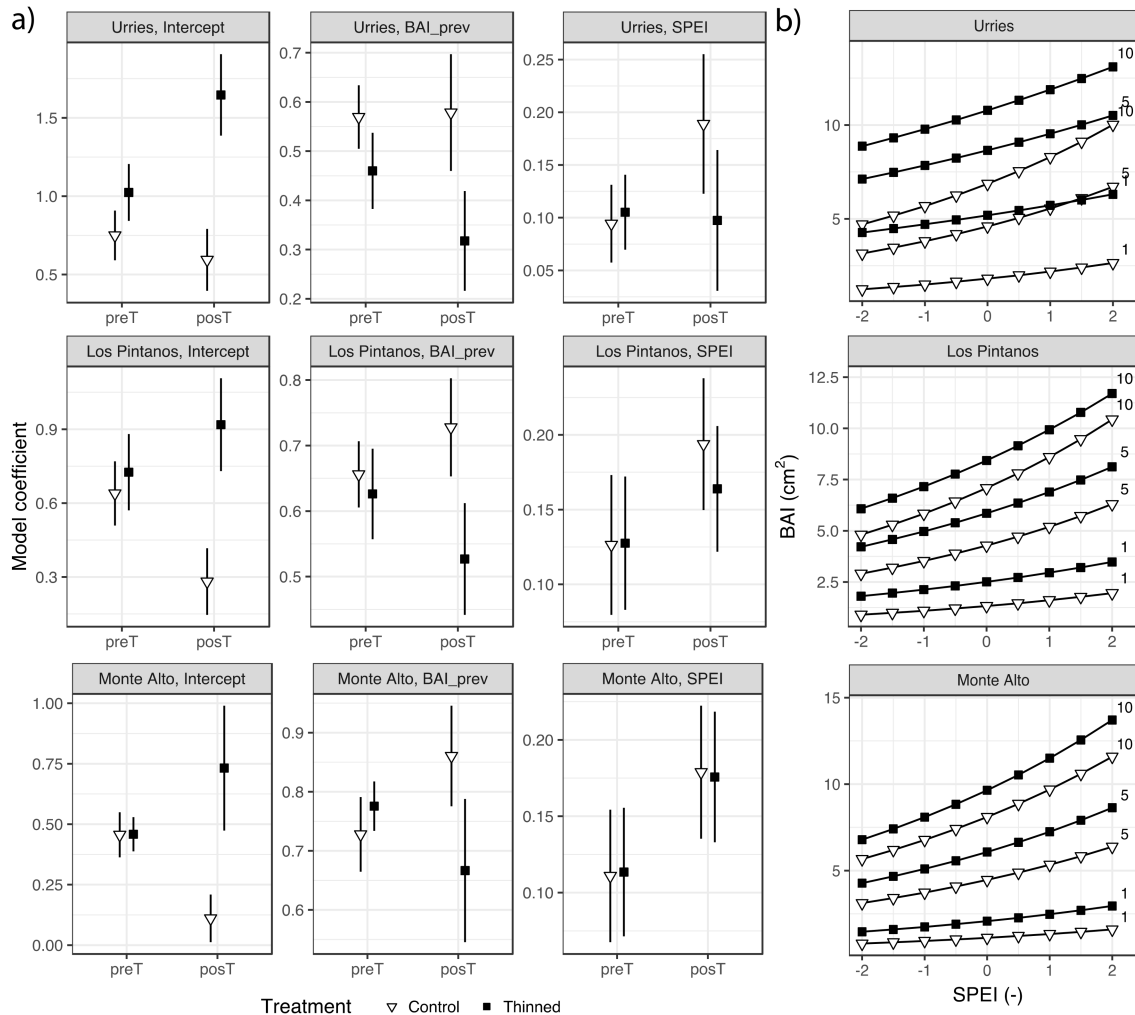


**Figure 3.** GLMM fixed-effects model coefficients (Bars depict 95% confidence intervals) for basal area increment (BAI) in Urriés, Los Pintanos and Monte Alto study sites in the thinned and control plots during pre- (*preT*) and post-thinning (*postT*) periods (a), and predicted BAI as a function of SPEI in the *postT* period for different values of previous growth,  $BAI_{prev}$  (1, 5 and 10 cm<sup>2</sup>) (b).

The model coefficients for  $BAI_{prev}$  were positive and significant ( $p < 0.05$ ), indicating a certain amount of autocorrelation in the BAI series. That is, the potential growth in a given year was positively influenced by the previous year's growth. There were no differences in the model coefficients between control and thinned plots before thinning (*preT* period). However, in the post-thinning (*postT*) period, the differences became more prominent and significant. While the influence of the previous year's BAI on growth increased or remained at a similar level than before the intervention in the control plots, it decreased in the thinned plots, indicating reduced dependence from the previous year's growth after thinning.

The model coefficients for SPEI were also positive in all cases, as expected (as positive values of SPEI indicate humid conditions associated with enhanced growth). The coefficients were similar between treatments in the *preT* period at all sites. In the *postT* period, the

coefficients were slightly lower in the thinned plots, but the difference was not significant. Overall, the effect of SPEI tended to be larger in the *posT* than in the *preT* period.

The results confirmed the importance of accounting for the effects of both temporal autocorrelation of BAI and climate. The model intercepts, which indicate the mean BAI under average  $BAI_{prev}$  and SPEI, showed non-significant differences between thinning and control plots in the *preT* period. However, differences arose in the *posT* period. Thus, while mean BAI tended to decrease in the control plots (significantly so in the Los Pintanos and Monte Alto sites), it experienced a relevant increase in the thinned plots (significantly so in Urriés). After thinning, the mean BAI increase was around 1–1.6  $cm^2$  in Urriés, 0.75–1  $cm^2$  in Los Pintanos, and 0.45–0.80  $cm^2$  in Monte Alto.

Figure 3b shows the predicted BAI in the *posT* period for different values of SPEI and  $BAI_{prev}$ . The differences in BAI between treatments are apparent. In all sites, growth was higher in the thinned plots for the same values of SPEI and  $BAI_{prev}$ . The highest variations among treatments were found in Urriés.

### 3.3. Thinning and Climate Effects on $WUE_i$ and $\delta^{18}O$

The examination of the  $WUE_i$  and  $\delta^{18}O$  time series revealed some interesting patterns (Figure 4).  $WUE_i$  exhibited a progressive increase during the whole period and for both treatments, especially during dry years. However,  $\delta^{18}O$  remains unchanged if not diminished (in Monte Alto), especially during the *posT* period.

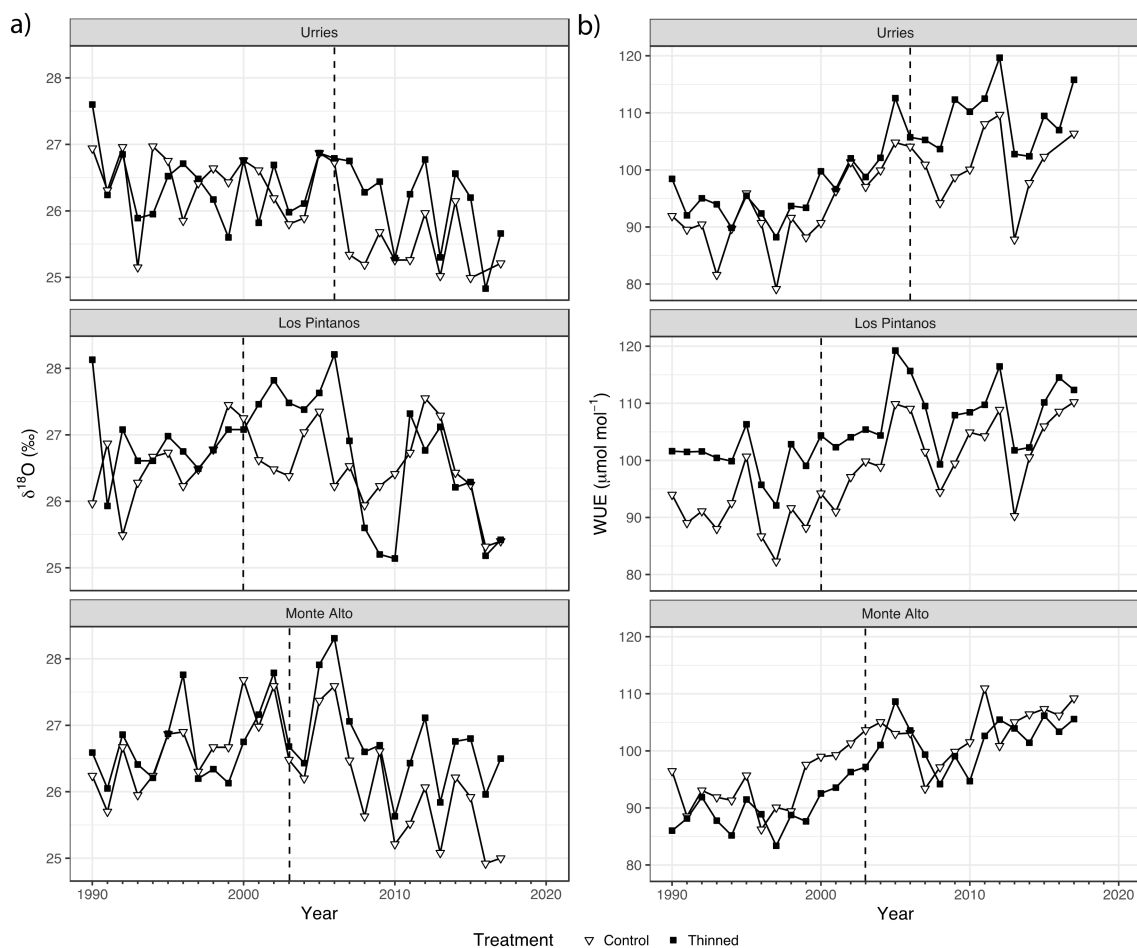


**Figure 4.** Time series of  $\delta^{18}O$  (a) and the intrinsic water-use efficiency ( $WUE_i$ , (b)) in Urriés, Los Pintanos, and Monte Alto study sites: control (white triangles) and thinning (black squares). The dashed vertical lines represent thinning treatments (2006, 2000, and 2003 in Urriés, Los Pintanos, and Monte Alto).

In all sites, the highest correlation between WUE and SPEI occurred at the time scale of 6 months and week 38 of the year (Figure S2), with negative and significant ( $p < 0.05$ ) correlations of  $-0.604$  in Urriés,  $-0.536$  in Los Pintanos, and  $-0.484$  in Monte Alto.

Results of the regression analysis of WUE<sub>i</sub> are shown in Figure 5a and Table S3. The SPEI negatively influenced WUE<sub>i</sub>, suggesting improved water use efficiency during dry periods vs humid ones. The model coefficients for SPEI were not always significant, as the confidence intervals overlapped the zero value, especially in Monte Alto. No differences were found in the SPEI model coefficients among treatments, *preT* and *postT* periods, and the three sites.

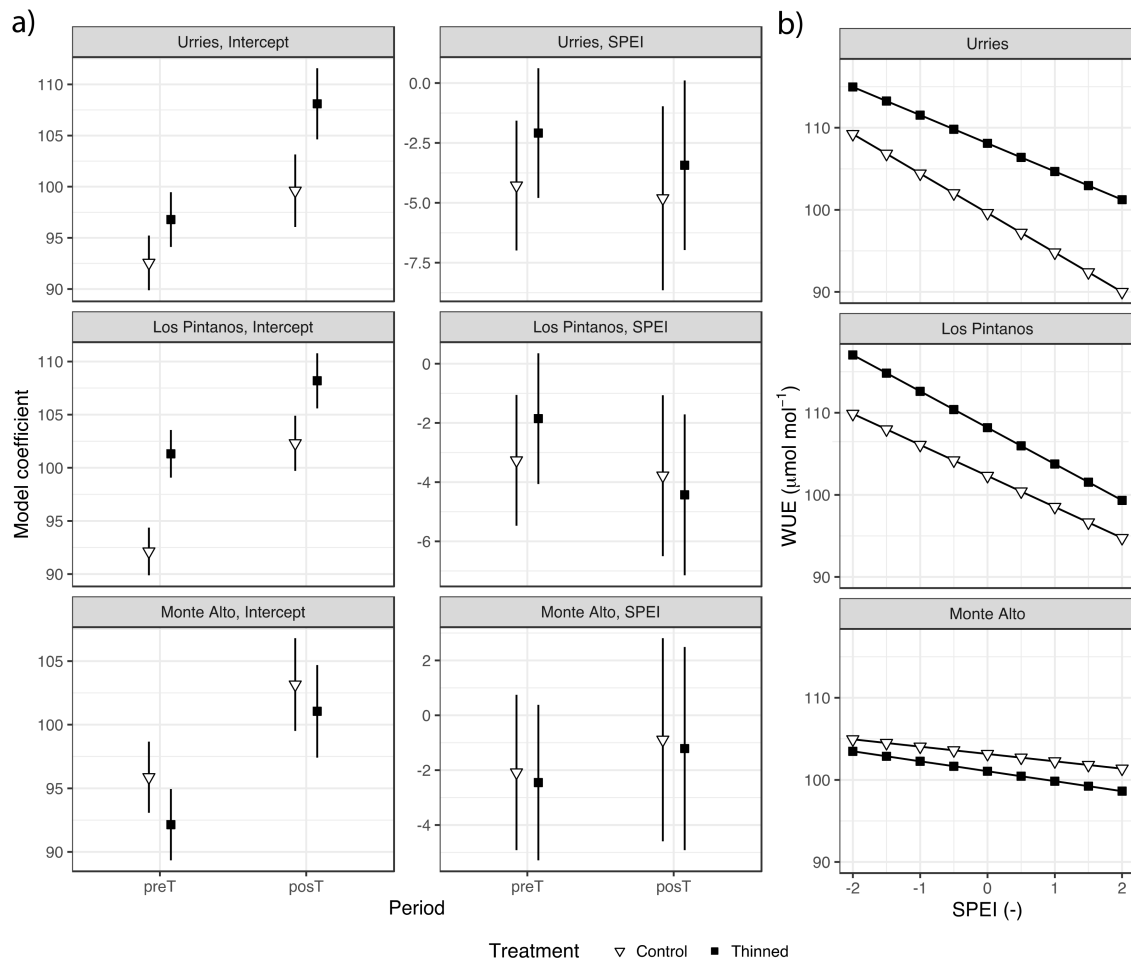


**Figure 5.** Intrinsic water use efficiency (WUE<sub>i</sub>), mean values model coefficients for the fixed effects (bars depict 95% confidence intervals) in Urriés, Los Pintanos and Monte Alto sites, for control and thinning treatments during pre- (*preT*) and post-thinning (*postT*) periods (a), and generalised linear models of WUE<sub>i</sub> against SPEI for the two treatments in the *postT* period (b).

Regarding the model intercepts, there were some differences during the *preT* period, only significant in Los Pintanos. The intercept increased significantly in the *postT* period in the two plots (thinned and control) and the three sites. The increase was higher in the thinned plots, with significant differences concerning control in Urriés and Los Pintanos (Table S3).

The relation between WUE<sub>i</sub> and SPEI for the *postT* period in control and thinned plots is depicted in Figure 5b. The highest WUE<sub>i</sub> occurred in the thinned plots, except in Monte Alto. In Urriés and Los Pintanos, WUE<sub>i</sub> ranged roughly between 115 and 90 μmol mol<sup>-1</sup> for dry and wet conditions, respectively, while in Monte Alto the range of WUE<sub>i</sub> variation was narrower.

Regarding  $\delta^{18}\text{O}$ , the highest correlation with SPEI was found at the time scale of 3 months and week 12 (Figure S2), with a negative significant correlation coefficient of  $-0.602$  in Urriés,  $-0.311$  in Los Pintanos, and  $-0.400$  in Monte Alto. Regression analysis showed a negative relation between  $\delta^{18}\text{O}$  and SPEI in general, meaning that  $\delta^{18}\text{O}$  tended to decrease during wet years and increased during droughts. However, the coefficients were not significant in all cases (Figure 6 and Table S4). The SPEI coefficients tended to decrease in the *postT* period, with no significant differences between treatments. Regarding the model intercepts, they tended to decrease during the *postT* period in the control plots (significantly so in Urriés and Monte Alto sites) while, in the thinned plots, they remained unchanged (Urriés) or also diminished (not significantly). The differences between treatments were only significant in Urriés during the *postT* period.

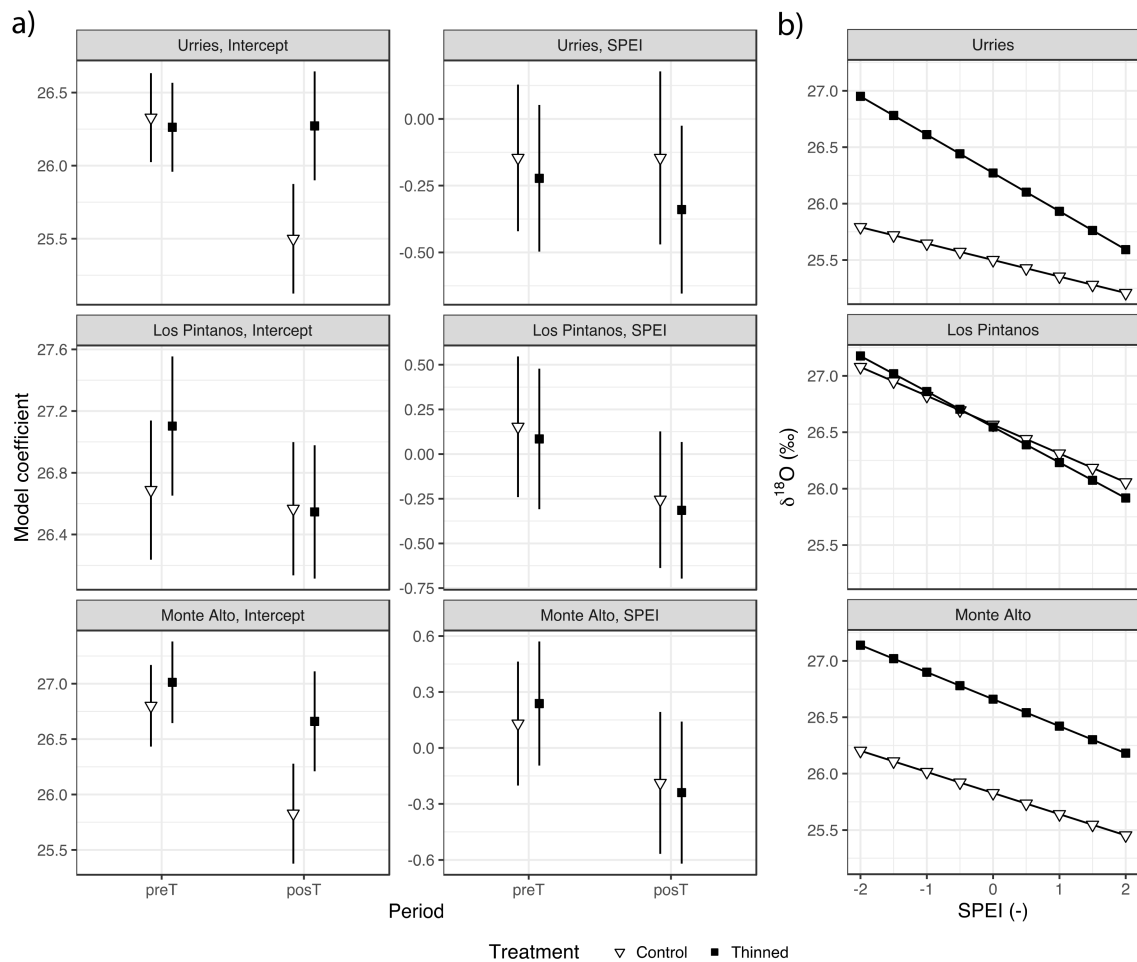


**Figure 6.**  $\delta^{18}\text{O}$  mean model coefficients for the values of the fixed effects (Bars depict 95% confidence intervals) in Urriés, Los Pintanos and Monte Alto study sites, for the two treatments and pre- (*preT*) and post-thinning (*postT*) periods (a), and generalised linear models of  $\delta^{18}\text{O}$  versus SPEI for both treatments only in the *postT* period (b).

The greater sensitivity of  $\delta^{18}\text{O}$  to SPEI in Urriés is depicted by the sharper response curve of thinned trees (Figure 6b). Therefore, during wet years (high SPEI values), the difference in  $\delta^{18}\text{O}$  concerning control was slight, but the difference increased rapidly as drought conditions were achieved. These results indicate a more flexible reaction of thinned trees to the climatic conditions on Urriés, although this difference was not significant. The rate of change of  $\delta^{18}\text{O}$  with SPEI was resemblant in all sites, changing between ca. 25‰ to 27‰.

### 3.4. Physiological Interpretations

Scheidegger et al. [24] offer an explanatory approach in the dual-isotope model to understand the variations in isotopic concentrations. In Figure 7, we interpret the annual and mean relative changes in  $\delta^{13}\text{C}$  and  $\delta^{18}\text{O}$  relative to the control plot ( $\Delta\delta^{13}\text{C}$  and  $\Delta\delta^{18}\text{O}$ , respectively) after thinning. As the starting point (white squares), we used the mean difference between thinned and control plots before thinning. In Urriés and Monte Alto, the primary signal was a positive shift along the  $\Delta\delta^{18}\text{O}$  axis. At the same time, there was more variability between years along the  $\Delta\delta^{13}\text{C}$  axis, and the average difference was also positive. In the Los Pintanos site, the primary signal was a negative shift in the  $\Delta\delta^{18}\text{O}$  axis and a positive shift in the  $\Delta\delta^{13}\text{C}$ . There was no connection between different climatic conditions and the positive or negative sign of  $\Delta\delta^{13}\text{C}$ .

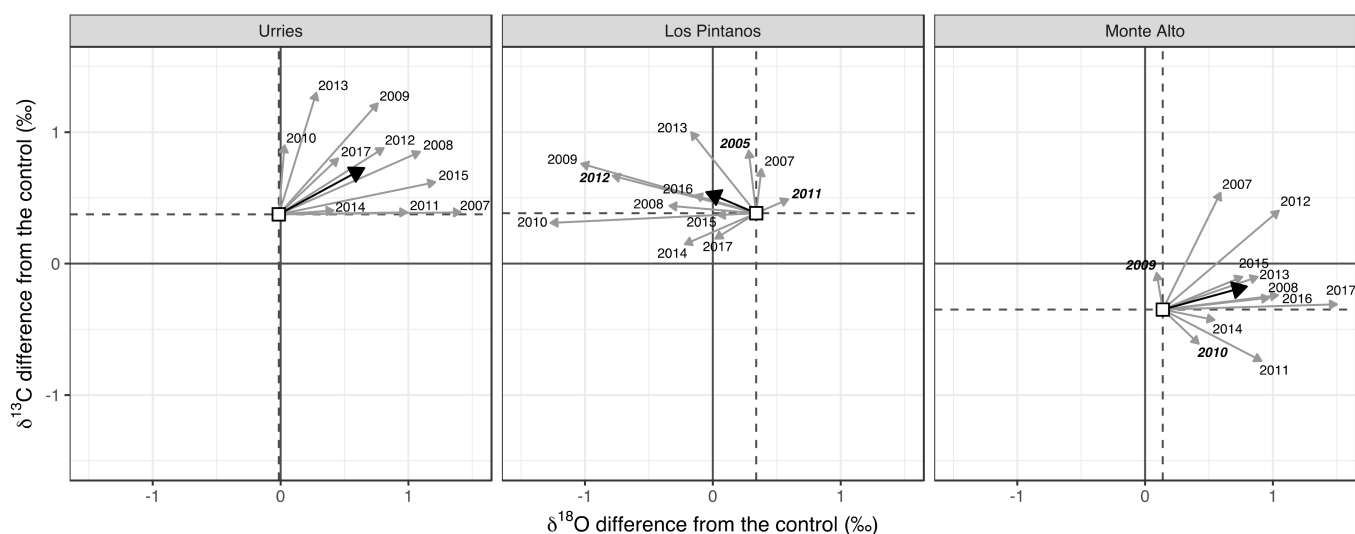


**Figure 7.** Annual and mean differences of  $\delta^{13}\text{C}$  and  $\delta^{18}\text{O}$  for modelled values concerning the control. White squares depict the mean values of  $\delta^{13}\text{C}$  and  $\delta^{18}\text{O}$  for the pre-thinning (*preT*) period. Grey arrows represent the changes in respect to the means for all years in the post-thinning (*posT*) period, and the black arrow depicts the mean value of the *posT* period. Dry years are indicated in bold typeface.

## 4. Discussion

The main goals of this study were to determine the effect of thinning on tree growth and to understand the physiological mechanisms of adaptation (water use and gas exchange) as tools to manage high-density pine plantations growing in the Mediterranean, seasonally dry regions. We analysed time series of radial growth (BAI), reconstructed intrinsic water-use efficiency (WUEi) and measured wood O isotope composition ( $\delta^{18}\text{O}$ ), and we related them to the hydric conditions during the growing season (SPEI) in thinned and control plots at three sites with similar environmental conditions.

### 4.1. Thinning Effects on Radial Growth

Thinning had an overall positive effect, as it improved growth in all sites. This result was expected, as thinning reduces competition among trees [2,12,48,49]. Our results are consistent with data obtained in previous thinning experiments in Black pine [2,3,20]. However, in addition to those earlier studies, our results confirm that thinning effects persisted for at least 13–14 years. Another study in two *Pinus halepensis* plantations showed thinning improved growth even 20 years after the thinning [28]. It is essential to evaluate the impact of thinning in long-term trials to assess the persistence of the management practices. Long-term thinning effects have been reported already for several pine species, such as Lodgepole pine (*Pinus contorta*), where the growth increase was sustained for 18 years [15], for 15 years in Maritime pine (*Pinus pinaster*) [14] after heavy thinning, and

for 29 years in Scots pine (*Pinus sylvestris*) [50]. For Black pine, growth amplification lasted for 12 years after thinning [2], and in short-term trials of 5–10 years in [20].

We also found that thinning reduced the BAI sensitivity to SPEI, with regression coefficients closer to zero. Lower climate sensitivity translates into reduced stress during drought, resulting in significant positive repercussions for growth, forest vigour, and health [51]. These results align with previous studies suggesting a feeble growth-climate relationship after thinning in *Pinus sylvestris* [12,50] and *P. halepensis* [52]. In Black pine, Martin-Benito et al. [2] detected that tree growth was less responsive to precipitation after thinning.

Another important finding was that the BAI dependence on the previous-year growth was reduced after thinning. These lines of evidence support the idea that thinned trees have a lower sensitivity to environmental stress, particularly to drought. Sánchez-Salguero et al. [3] arrived at similar conclusions for *P. nigra*, asserting that thinning of drought-prone planted forests decreases competition and enhances the adaptive capacity to withstand drought stress by increasing resilience and reducing vulnerability.

#### 4.2. Thinning Influence on Water Use Efficiency

The WUEi exhibited an increasing trend during the study period for both treatments in the three sites. As expected, WUEi increased primarily during dry years, when trees are affected by water scarcity [22]. This was also evident from the regression model results, as WUEi had a negative relationship with the SPEI consistently, indicating that lower water use efficiency is linked to relief in water stress [53].

In two sites, we found significant differences in WUEi between control and thinned plots after thinning. In the third site (Los Pintanos), there were differences between the plots before thinning. Other authors also found increasing WUEi after thinning, such as [14] in Mediterranean *P. pinaster* forests and [21] in Monterey pine (*Pinus radiata*), under more mesic conditions. However, others reported decreasing WUEi in pine species such as *P. sylvestris* [50], Ponderosa pine (*Pinus ponderosa*) [54], and *P. halepensis* [28,52], associated with drier, semiarid sites. Other authors reported no significant changes in WUEi in *P. nigra* [2] and *P. halepensis* [22]. Whereas the reaction of WUEi to thinning is variable, the large number of tree-ring isotope studies determined that a reduction in competition can enhance tree water availability and stomatal conductance and carbon assimilation, thereby decreasing drought stress via improved resilience [55].

When considering the effects of SPEI on WUEi under control and thinned plots, we did not find any differences between treatments during the *preT* and *postT* periods. This effect was constant across sites. It should also be noted that very wet conditions occurred in the post-thinning period 2013–2015 (Figure S3), which could have induced a passive physiological response characterised by a reduced impact of rising  $c_a$  on tree WUEi [51].

#### 4.3. Thinning Effects on C and O Isotope Composition and Physiological Interpretations

In Urriés and Monte Alto, the primary signal was a positive shift in both the  $\Delta\delta^{18}\text{O}$  and  $\Delta\delta^{13}\text{C}$  axes (Figure 7), while in Los Pintanos, the change along the  $\Delta\delta^{18}\text{O}$  axis was negative. According to the dual-isotope model of [24], the increase of  $\delta^{18}\text{O}$  and  $\delta^{13}\text{C}$  in Urriés and Monte Alto of thinned trees as compared to control trees need to be understood as a consequence of a decrease of stomatal conductance ( $g_s$ ) at constant photosynthetic capacity ( $A$ ). On the other hand, in Los Pintanos, the reduction of  $\delta^{18}\text{O}$  and increase of  $\delta^{13}\text{C}$  should correspond to constant  $g_s$  with increasing  $A$ .

Nevertheless, according to Barnard et al. [27], caution should always be used when interpreting physiological responses from the dual-isotope conceptual model. The interpretation of  $\delta^{18}\text{O}$  remains unclear since variation can be produced through several mechanisms [56,57]. The  $\delta^{18}\text{O}$  of plant material can be affected by differences in  $\delta^{18}\text{O}$  of source water and variations in  $\delta^{18}\text{O}$  of water vapour [56,58]. In addition, several reports have shown that when plants share water sources, variation in  $\delta^{18}\text{O}$  is strongly correlated with relative humidity and evaporative demand, which influence  $g_s$  [25,27,59–61]. As

differences in air humidity and vapour pressure deficit have a substantial effect on  $\delta^{18}\text{O}$  enrichment, variation between plots could make the interpretation of results problematic [26]. What is more, according to [27], changes in air humidity drive changes in  $\delta^{18}\text{O}$  and influence  $g_s$ .

It could be hypothesised that a variation of air humidity is likely to occur after thinning. Removal of a significant number of trees produces a hotter micro-climate with enhanced turbulence and air interchange at the forest stand level, resulting in a lower air humidity [2,62]. Consequently, the  $\delta^{18}\text{O}$  enrichment detected could not be associated with changes in stomatal conductance rates. Other authors have put forward this mechanism [2,52] and in our previous study on *P. halepensis* [28]. This observation may support the hypothesis that the increase of WUEi observed in Urriés and Monte Alto after thinning could potentially be an effect of enhanced light or nitrogen availability (which would strengthen WUEi) in contradiction to the influence of enhanced soil moisture (which would decrease WUEi) [54]. Under that hypothesis, the increase of interception of radiation by trees in the thinned plots should be associated with increased rates of photosynthesis ( $A$ ) [21]. In Los Pintanos, the decrease of  $\delta^{18}\text{O}$  and increase of  $\delta^{13}\text{C}$  should be interpreted as variations of both  $A$  and  $g_s$ , with the former being proportionally larger than the latter. This suggests that the thinning effect on this site could have something to do with an increase of light, along with an increase of soil moisture per tree. The difference between Los Pintanos and the other two sites could be related to the much higher tree density before and after thinning, resulting in increased competition for resources. These results match previous studies where larger changes in  $A$  than  $g_s$  or unchanged  $g_s$  were detected [21,63,64]. These studies were conducted in mesic to wet areas, where water is less limiting than in our study sites [50].

These findings may help us understand the variable reaction of WUEi to thinning. A possible explanation for this might be the different hydrologic balance from mesic to xeric sites. This has been evident in the case of our previous work [28] carried out on two semiarid *P. halepensis* sites with a mean hydrologic balance (annual precipitation minus potential evapotranspiration) of  $-720$  mm. In the two sites analysed, WUEi decreased in the thinned plots, which we interpreted as a sign of relieving drought stress. Similar results were found in other studies associated with xeric conditions [50,52,54].

#### 4.4. Other Issues

Our work focuses on the ecological effects of thinning, particularly regarding the competence for resources, and leaves many other topics not treated. In particular, we did not consider how thinning may affect productivity and yield at the stand level. It has been claimed that thinning can harm stand productivity in the long term due to decreased tree density [16]. However, this is highly site- and species-specific. Stand productivity after thinning depends on the combined effect of the thinning intensity (number of trees logged) and the growth boost to the remaining trees. Trees in rich vs poor sites (from climatic and other environmental points of view) may also react differently. Also, the thinning strategy (thinning from below vs thinning from above) may have a relevant influence on the thinning effects [65].

In addition, thinning may also have other ecological effects that might be considered, such as the higher wind speeds in recently thinned stands that could lead to a risk of felling, the greater penetration of solar radiation [65] and the increase of understory vegetation [66]. On the other hand, thinning might have a positive effect in facing biotic disturbances, as it has been shown that higher resource acquisition capacity per tree can reduce predisposition to insect plagues and diseases [67].

## 5. Conclusions

Thinning enhanced growth but, more importantly, also decreased growth sensitivity to climate and reduced year-to-year growth dependence. Lastly, the water use efficiency also increased in response to thinning. These effects remained at least 13–14 years after

thinning. As an appropriate management strategy, our results recommend that a thinning treatment (40% of the initial stand basal area removed) can be an instrument to adapt the Mediterranean and other seasonally dry pine forests and plantations to climate variability.

**Supplementary Materials:** The following are available online at <https://www.mdpi.com/article/10.3390/f12080985/s1>, Figure S1: Ombrothermic diagrams showing the mean monthly distribution of temperature (dashed line) and precipitation (grey bars) at Urriés (a), Los Pintanos (b) and Monte Alto (c) study sites. Figure S2: Correlations between BAI,  $\delta^{18}\text{O}$  and WUEi time series and SPEI time series at various time scales (y-axis) and weeks of the year (x-axis). Significant correlations are indicated with a dot, and the maximum significant correlation for each case is marked with a circle. Correlation between BAI and SPEI in Urriés (significant at week 42, 6-month SPEI) (a), BAI and SPEI in Los Pintanos (significant at week 37, 9-month) (b), BAI and SPEI in Monte Alto (significant at week 37, 12-month SPEI) (c),  $\delta^{18}\text{O}$  and SPEI in Urriés, Los Pintanos and Monte Alto (significant at week 12, 3-month SPEI) (d), WUEi and SPEI in Urriés, Los Pintanos and Monte Alto (significant at week 38, 6-month SPEI) (e). Figure S3: SPEI time series at 6-month and 42-week time scale for Urriés, 9-month time scale week 37 in Los Pintanos and 12-months 37-week in Monte Alto study sites. Solid vertical lines indicate the year of thinning at each location. Red and blue bars indicate dry and wet conditions, respectively. Table S1: Tree-ring width statistics. Table S2: Summary of the linear models of the effect of thinning on growth (BAI) on Urriés, Los Pintanos and Monte Alto study sites. The periods correspond to the pre- (*preT*) and post-thinning (*postT*) periods. Table S3: Summary of the linear models of the effect of thinning on WUEi values on Urriés, Los Pintanos and Monte Alto study sites. The periods correspond to the pre- (*preT*) and post-thinning (*postT*) periods. Table S4: Summary of the linear models of thinning effect on  $\delta^{18}\text{O}$  values on Urriés, Los Pintanos and Monte Alto study sites. The periods correspond to the pre- (*preT*) and post-thinning (*postT*) periods.

**Author Contributions:** Conceptualization, À.M.-A., S.B. and J.J.C.; methodology, S.B. and J.J.C.; formal analysis, S.B.; investigation, À.M.-A.; data curation, M.T.-B.; writing—original draft preparation, À.M.-A.; writing—review and editing, S.B. and J.J.C.; supervision, S.B.; funding acquisition, S.B. All authors have read and agreed to the published version of the manuscript.

**Funding:** Funding for this research was provided by the “Agencia Estatal de Investigación” of Spain (CSIC) in the frame of the ERA-NET WaterWorks2015 co-funded Call (project PCIN-2017-020/INNOMED). This ERA-NET is an integral part of the 2016 Joint Activities developed by the Water Challenges for a Changing World Joint Programme Initiative (Water JPI) as a result of a joint collaborative effort with the Joint Programming Initiative on Agriculture, Food Security and Climate Change (FACCE JPI). Funding was also provided by the project EFA210/16/PIRAGUA, co-funded by the European Regional Development Fund (ERDF) through the Interreg V Spain-France-Andorre Programme (POCTEFA 2014-2020) of the European Union. The authors also acknowledge support from the Spanish Ministry of Science, Innovation and Universities through the research projects FORMAL (RTI2018-096884-B-C31) and CLICES (CGL2017-83866-C3-3-R).

**Institutional Review Board Statement:** Not applicable.

**Informed Consent Statement:** Not applicable.

**Data Availability Statement:** Data available for research upon request.

**Acknowledgments:** We sincerely thank E. Arrechea and Alvaro Hernández (Gob. Aragón) for their support and help to study Urriés, Los Pintanos and Monte Alto study sites.

**Conflicts of Interest:** The authors declare no conflict of interest. The funders had no role in the design of the study; in the collection, analyses, or interpretation of data; in the writing of the manuscript, or in the decision to publish the results.

## References

1. Giorgi, F.; Lionello, P. Climate change projections for the Mediterranean region. *Glob. Planet. Chang.* **2008**, *63*, 90–104. [[CrossRef](#)]
2. Martín-Benito, D.; del Río, M.; Heinrich, I.; Helle, G.; Cañellas, I. Response of climate-growth relationships and water use efficiency to thinning in a *Pinus nigra* afforestation. *For. Ecol. Manag.* **2010**, *259*, 967–975. [[CrossRef](#)]
3. Sánchez-Salguero, R.; Camarero, J.J.; Dobbertin, M.; Fernández-Cancio, Á.; Vilà-Cabrera, A.; Manzanedo, R.D.; Zavala, M.A.; Navarro-Cerrillo, R.M. Contrasting vulnerability and resilience to drought-induced decline of densely planted vs. natural rear-edge *Pinus nigra* forests. *For. Ecol. Manag.* **2013**, *310*, 956–967. [[CrossRef](#)]

4. Gazol, A.; Camarero, J.J.; Sangüesa-Barreda, G.; Serra-Maluquer, X.; Sánchez-Salguero, R.; Coll, L.; Casals, P. Tree Species Are Differently Impacted by Cumulative Drought Stress and Present Higher Growth Synchrony in Dry Places. *Front. For. Glob. Chang.* **2020**, *3*. [[CrossRef](#)]
5. Sánchez-Salguero, R.; Linares, J.C.; Camarero, J.J.; Madrigal-González, J.; Hevia, A.; Sánchez-Miranda, A.; Ballesteros-Cánovas, J.A.; Sánchez, R.A.; García-Cervigón, A.I.; Bigler, C.; et al. Disentangling the effects of competition and climate on individual tree growth: A retrospective and dynamic approach in Scots pine. *For. Ecol. Manag.* **2015**, *358*, 12–25. [[CrossRef](#)]
6. Tague, C.L.; Moritz, M.; Hanan, E. The changing water cycle: The eco-hydrologic impacts of forest density reduction in Mediterranean (seasonally dry) regions. *Wiley Interdiscip. Rev. Water* **2019**, e1350. [[CrossRef](#)]
7. D’Amato, A.W.; Bradford, J.B.; Fraver, S.; Palik, B.J. Effects of thinning on drought vulnerability and climate response in north temperate forest ecosystems. *Ecol. Appl.* **2013**, *23*, 1735–1742. [[CrossRef](#)] [[PubMed](#)]
8. Tarancón, A.A.; Fulé, P.Z.; Shive, K.L.; Sieg, C.H.; Meador, A.S.; Strom, B. Simulating post-wildfire forest trajectories under alternative climate and management scenarios. *Ecol. Appl.* **2014**, *24*, 1626–1637. [[CrossRef](#)]
9. Schmitt, A.; Trouvé, R.; Seynave, I.; LeBourgeois, F. Decreasing stand density favors resistance, resilience, and recovery of *Quercus petraea* trees to a severe drought, particularly on dry sites. *Ann. For. Sci.* **2020**, *77*, 1–21. [[CrossRef](#)]
10. Molina, A.J.; del Campo, A.D. The effects of experimental thinning on throughfall and stemflow: A contribution towards hydrology-oriented silviculture in Aleppo pine plantations. *For. Ecol. Manag.* **2012**, *269*, 206–213. [[CrossRef](#)]
11. Pretzsch, H.; Schütze, G.; Biber, P. Drought can favour the growth of small in relation to tall trees in mature stands of Norway spruce and European beech. *For. Ecosyst.* **2018**, *5*, 20. [[CrossRef](#)]
12. Sohn, J.A.; Saha, S.; Bauhus, J. Potential of forest thinning to mitigate drought stress: A meta-analysis. *For. Ecol. Manag.* **2016**, *380*, 261–273. [[CrossRef](#)]
13. Del Campo, A.D.; Fernandes, T.J.; Molina, A.J. Hydrology-oriented (adaptive) silviculture in a semiarid pine plantation: How much can be modified the water cycle through forest management? *Eur. J. For. Res.* **2014**, *133*, 879–894. [[CrossRef](#)]
14. Navarro-Cerrillo, R.; Sánchez-Salguero, R.; Herrera, R.; Ruiz, C.C.; Moreno-Rojas, J.; Manzanedo, R.D.; López-Quintanilla, J. Contrasting growth and water use efficiency after thinning in mixed *Abies pinsapo*–*Pinus pinaster*–*Pinus sylvestris* forests. *J. For. Sci.* **2016**, *62*, 53–64.
15. Prescott, C.; de Montigny, L.; Harper, G. Eighteen-year growth responses to thinning and fertilization of a height-repressed lodgepole pine stand in interior British Columbia. *For. Chron.* **2019**, *95*, 207–221. [[CrossRef](#)]
16. Steckel, M.; Moser, W.K.; Del Río, M.; Pretzsch, H. Implications of Reduced Stand Density on Tree Growth and Drought Susceptibility: A Study of Three Species under Varying Climate. *Forests* **2020**, *11*, 627. [[CrossRef](#)]
17. McDowell, N.G.; Adams, H.D.; Bailey, J.D.; Hess, M.; Kolb, T.E. Homeostatic maintenance of ponderosa pine gas exchange in response to stand density changes. *Ecol. Appl.* **2006**, *16*, 1164–1182. [[CrossRef](#)]
18. McCarroll, D.; Loader, N. Stable isotopes in tree rings. *Quat. Sci. Rev.* **2004**, *23*, 771–801. [[CrossRef](#)]
19. Gessler, A.; Cailleret, M.; Joseph, J.; Schönbeck, L.; Schaub, M.; Lehmann, M.; Treydte, K.; Rigling, A.; Timofeeva, G.; Saurer, M. Drought induced tree mortality—A tree-ring isotope based conceptual model to assess mechanisms and predispositions. *New Phytol.* **2018**, *219*, 485–490. [[CrossRef](#)]
20. Navarro-Cerrillo, R.M.; Sánchez-Salguero, R.; Rodríguez, C.; Lazo, J.D.; Moreno-Rojas, J.M.; Palacios-Rodríguez, G.; Camarero, J.J. Is thinning an alternative when trees could die in response to drought? The case of planted *Pinus nigra* and *P. sylvestris* stands in southern Spain. *For. Ecol. Manag.* **2019**, *433*, 313–324. [[CrossRef](#)]
21. Warren, C.R.; McGrath, J.F.; Adams, M. Water availability and carbon isotope discrimination in conifers. *Oecologia* **2001**, *127*, 476–486. [[CrossRef](#)]
22. Moreno-Gutiérrez, C.; Battipaglia, G.; Cherubini, P.; Saurer, M.; Nicolas, E.; Contreras, S.; Querejeta, J.I. Stand structure modulates the long-term vulnerability of *Pinus halepensis* to climatic drought in a semiarid Mediterranean ecosystem. *Plant Cell Environ.* **2012**, *35*, 1026–1039. [[CrossRef](#)]
23. Fernández-De-Uña, L.; McDowell, N.G.; Cañellas, I.; Gea-Izquierdo, G. Disentangling the effect of competition, CO<sub>2</sub> and climate on intrinsic water-use efficiency and tree growth. *J. Ecol.* **2016**, *104*, 678–690. [[CrossRef](#)]
24. Scheidegger, Y.; Saurer, M.; Bahn, M.; Siegwolf, R. Linking stable oxygen and carbon isotopes with stomatal conductance and photosynthetic capacity: A conceptual model. *Oecologia* **2000**, *125*, 350–357. [[CrossRef](#)]
25. Barbour, M.M.; Fischer, R.A.; Sayre, K.D.; Farquhar, G.D. Oxygen isotope ratio of leaf and grain material correlates with stomatal conductance and grain yield in irrigated wheat. *Funct. Plant Biol.* **2000**, *27*, 625. [[CrossRef](#)]
26. Roden, J.; Siegwolf, R. Is the dual-isotope conceptual model fully operational? *Tree Physiol.* **2012**, *32*, 1179–1182. [[CrossRef](#)] [[PubMed](#)]
27. Barnard, H.; Brooks, J.; Bond, B. Applying the dual-isotope conceptual model to interpret physiological trends under uncontrolled conditions. *Tree Physiol.* **2012**, *32*, 1183–1198. [[CrossRef](#)]
28. Manrique-Alba, À.; Beguería, S.; Molina, A.J.; González-Sanchis, M.; Tomàs-Burguera, M.; Del Campo, A.D.; Colangelo, M.; Camarero, J.J. Long-term thinning effects on tree growth, drought response and water use efficiency at two Aleppo pine plantations in Spain. *Sci. Total Environ.* **2020**, *728*, 138536. [[CrossRef](#)]
29. Linares, J.C.; Tiscar, P.A. Climate change impacts and vulnerability of the southern populations of *Pinus nigra* subsp. *salzmannii*. *Tree Physiol.* **2010**, *30*, 795–806. [[CrossRef](#)] [[PubMed](#)]

30. Gazol, A.; Hernández-Alonso, R.; Camarero, J.J. Patterns and Drivers of Pine Processionary Moth Defoliation in Mediterranean Mountain Forests. *Front. Ecol. Evol.* **2019**, *7*. [[CrossRef](#)]
31. Vicente-Serrano, S.M.; Tomas-Burguera, M.; Beguería, S.; Reig-Gracia, F.; Latorre, B.; Peña-Gallardo, M.; Luna, M.Y.; Morata, A.; González-Hidalgo, J.C. A High Resolution Dataset of Drought Indices for Spain. *Data* **2017**, *2*, 22. [[CrossRef](#)]
32. Tomas-Burguera, M.; Vicente-Serrano, S.M.; Beguería, S.; Reig, F.; Latorre, B. Reference crop evapotranspiration database in Spain (1961–2014). *Earth Syst. Sci. Data* **2019**, *11*, 1917–1930. [[CrossRef](#)]
33. Köppen, W. IDas Geographischa System der Klimate. *Handbuchder Klimatologiei*. Köppen, W., Geiger, G., Eds.; 1936, pp. 1–44. Available online: [https://www.scrip.org/\(S\(czeh2tfqyw2orz553k1w0r45\)\)/reference/ReferencesPapers.aspx?ReferenceID=242388](https://www.scrip.org/(S(czeh2tfqyw2orz553k1w0r45))/reference/ReferencesPapers.aspx?ReferenceID=242388) (accessed on 20 May 2021).
34. World Reference Base for Soil Resources (WRB). *Update 2015. World Soil Resources Reports 106*; FAO: Rome, Italy, 2014.
35. Holmes, R.L. Computer-assisted quality control in tree-ring dating and measurement. *Tree-Ring Bull.* **1983**, *43*, 69–75.
36. Biondi, F.; Qeadan, F. A theory-driven approach to tree-ring standardization: Defining the biological trend from expected basal area increment. *Tree-Ring Res.* **2008**, *64*, 81–96. [[CrossRef](#)]
37. Vicente-Serrano, S.M.; Beguería, S.; López-Moreno, J.I. A multiscalar drought index sensitive to global warming: The standardized precipitation evapotranspiration index. *J. Clim.* **2010**, *23*, 1696–1718. [[CrossRef](#)]
38. Beguería, S.; Vicente-Serrano, S.M.; Reig, F.; Latorre, B. Standardized precipitation evapotranspiration index (SPEI) revisited: Parameter fitting, evapotranspiration models, tools, datasets and drought monitoring. *Int. J. Climatol.* **2014**, *34*, 3001–3023. [[CrossRef](#)]
39. Saurer, M.; Siegwolf, R.T.W.; Schweingruber, F.H. Carbon isotope discrimination indicates improving water-use efficiency of trees in northern Eurasia over the last 100 years. *Glob. Chang. Biol.* **2004**, *10*, 2109–2120. [[CrossRef](#)]
40. Belmecheri, S.; Lavergne, A. Compiled records of atmospheric CO<sub>2</sub> concentrations and stable carbon isotopes to reconstruct climate and derive plant ecophysiological indices from tree rings. *Dendrochronologia* **2020**, *63*, 125748. [[CrossRef](#)]
41. Farquhar, G.; Richards, R. Isotopic composition of plant carbon correlates with water-use efficiency of wheat genotypes. *Funct. Plant Biol.* **1984**, *11*, 539–552. [[CrossRef](#)]
42. Farquhar, G.; O’Leary, M.; Berry, J. On the Relationship between Carbon Isotope Discrimination and the Intercellular Carbon Dioxide Concentration in Leaves. *Funct. Plant Biol.* **1982**, *9*, 121–137. [[CrossRef](#)]
43. Francey, R.J.; Farquhar, G. An explanation of 13C/12C variations in tree rings. *Nature* **1982**, *297*, 28–31. [[CrossRef](#)]
44. Pinheiro, J.; Bates, D. *Mixed-Effects Models in S and S-PLUS*; Springer Science & Business Media: Berlin/Heidelberg, Germany, 2006.
45. Powell, M.J.D. *The BOBYQA Algorithm for Bound Constrained Optimisation without Derivatives*; Report No. DAMTP 2009/NA06; Centre for Mathematical Sciences, Univ.: Cambridge, UK, 2009; Available online: [http://www.damtp.cam.ac.uk/user/na/NA\\_papers/NA2009\\_06.pdf](http://www.damtp.cam.ac.uk/user/na/NA_papers/NA2009_06.pdf) (accessed on 22 May 2021).
46. Bates, D.; Mächler, M.; Bolker, B.; Walker, S. Fitting Linear Mixed-Effects Models Using lme4. *J. Stat. Softw.* **2015**, *67*, 1–48. [[CrossRef](#)]
47. R Core Team. *R: A Language and Environment for Statistical Computing*; R Foundation for Statistical Computing: Vienna, Austria, 2021; Available online: <https://www.R-project.org/> (accessed on 22 May 2021).
48. Breda, N.; Granier, A.; Aussenac, G. Effects of thinning on soil and tree water relations, transpiration and growth in an oak forest (*Quercus petraea* (Matt.) Liebl.). *Tree Physiol.* **1995**, *15*, 295–306. [[CrossRef](#)] [[PubMed](#)]
49. Vilà-Cabrera, A.; Coll, L.; Martínez-Vilalta, J.; Retana, J. Forest management for adaptation to climate change in the Mediterranean basin: A synthesis of evidence. *For. Ecol. Manag.* **2018**, *407*, 16–22. [[CrossRef](#)]
50. Giuggiola, A.; Ogee, J.; Rigling, A.; Gessler, A.; Bugmann, H.; Treydte, K. Improvement of water and light availability after thinning at a xeric site: Which matters more? A dual isotope approach. *New Phytol.* **2015**, *210*, 108–121. [[CrossRef](#)]
51. Linares, J.C.; Camarero, J.J. From pattern to process: Linking intrinsic water-use efficiency to drought-induced forest decline. *Glob. Chang. Biol.* **2011**, *18*, 1000–1015. [[CrossRef](#)]
52. Fernandes, T.J.; del Campo, A.; Herrera, R.; Molina, A.J. Simultaneous assessment, through sap flow and stable isotopes, of water use efficiency (WUE) in thinned pines shows improvement in growth, tree-climate sensitivity and WUE, but not in WUEi. *For. Ecol. Manag.* **2016**, *361*, 298–308. [[CrossRef](#)]
53. Klein, T.; Hemming, D.; Lin, T.; Grünzweig, J.M.; Maseyk, K.; Rotenberg, E.; Yakir, D. Association between tree-ring and needle δ<sup>13</sup>C and leaf gas exchange in *Pinus halepensis* under semi-arid conditions. *Oecologia* **2005**, *144*, 45–54. [[CrossRef](#)]
54. McDowell, N.; Brooks, J.R.; Fitzgerald, S.A.; Bond, B.J. Carbon isotope discrimination and growth response of old *Pinus ponderosa* trees to stand density reductions. *Plant Cell Environ.* **2003**, *26*, 631–644. [[CrossRef](#)]
55. Sohn, J.A.; Gebhardt, T.; Ammer, C.; Bauhus, J.; Häberle, K.-H.; Matyssek, R.; Grams, T.E. Mitigation of drought by thinning: Short-term and long-term effects on growth and physiological performance of Norway spruce (*Picea abies*). *For. Ecol. Manag.* **2013**, *308*, 188–197. [[CrossRef](#)]
56. Farquhar, G.D.; Barbour, M.M.; Henry, B.K. Interpretation of oxygen isotope composition of leaf material. In *Stable Isotopes: Integration of Biological, Ecological and Geochemical Processes*; Griffiths, H., Ed.; BIOS Scientific Publishers: Oxford, UK, 1998; pp. 27–61.
57. Barbour, M.M. Stable oxygen isotope composition of plant tissue: A review. *Funct. Plant Biol.* **2007**, *34*, 83–94. [[CrossRef](#)]

58. Roden, J.S.; Lin, G.; Ehleringer, J.R. A mechanistic model for interpretation of hydrogen and oxygen isotope ratios in tree-ring cellulose. *Geochim. Cosmochim. Acta* **2000**, *64*, 21–35. [[CrossRef](#)]
59. Barbour, M.; Farquhar, G. Relative humidity-and ABA-induced variation in carbon and oxygen isotope ratios of cotton leaves. *Plant Cell Environ.* **2000**, *23*, 473–485. [[CrossRef](#)]
60. Siegwolf, R.T.W.; Matyssek, R.; Saurer, M.; Maurer, S.; Günthardt-Goerg, M.S.; Schmutz, P.; Bucher, J.B. Stable isotope analysis reveals differential effects of soil nitrogen and nitrogen dioxide on the water use efficiency in hybrid poplar leaves. *New Phytol.* **2001**, *149*, 233–246. [[CrossRef](#)] [[PubMed](#)]
61. Roden, J.S.; Farquhar, G.D. A controlled test of the dual-isotope approach for the interpretation of stable carbon and oxygen isotope ratio variation in tree rings. *Tree Physiol.* **2012**, *32*, 490–503. [[CrossRef](#)] [[PubMed](#)]
62. Anderson, P.D.; Larson, D.J.; Chan, S.S. Riparian buffer and density management influences on microclimate of young headwater forests of western Oregon. *For. Sci.* **2007**, *53*, 254–269.
63. Powers, M.D.; Pregitzer, K.S.; Palik, B.J.; Webster, C.R. Wood  $\delta^{13}\text{C}$ ,  $\delta^{18}\text{O}$  and radial growth responses of residual red pine to variable retention harvesting. *Tree Physiol.* **2010**, *30*, 326–334. [[CrossRef](#)] [[PubMed](#)]
64. Brooks, J.R.; Mitchell, A.K. Interpreting tree responses to thinning and fertilization using tree-ring stable isotopes. *New Phytol.* **2011**, *190*, 770–782. [[CrossRef](#)]
65. Pretzsch, H. Density and growth of forest stands revisited. Effect of the temporal scale of observation, site quality, and thinning. *For. Ecol. Manag.* **2020**, *460*, 117879. [[CrossRef](#)]
66. Thomas, S.C.; Halpern, C.B.; Falk, D.A.; Liguori, D.A.; Austin, K.A. Plant diversity in managed forests: Understory responses to thinning and fertilization. *Ecol. Appl.* **1999**, *9*, 864–879. [[CrossRef](#)]
67. Chmura, D.J.; Anderson, P.D.; Howe, G.T.; Harrington, C.A.; Halofsky, J.E.; Peterson, D.L.; Shaw, D.C.; St. Clair, J.B. Forest responses to climate change in the northwestern United States: Ecophysiological foundations for adaptive management. *For. Ecol. Manag.* **2011**, *261*, 1121–1142. [[CrossRef](#)]